



## Morphology and swelling of thin films of dialcohol xylan

Downloaded from: <https://research.chalmers.se>, 2025-12-04 23:33 UTC

Citation for the original published paper (version of record):

Palasingh, C., Kargl, R., Stana Kleinschek, K. et al (2023). Morphology and swelling of thin films of dialcohol xylan. Carbohydrate Polymers, 313. <http://dx.doi.org/10.1016/j.carbpol.2023.120810>

N.B. When citing this work, cite the original published paper.



# Morphology and swelling of thin films of dialcohol xylan

Chonnipa Palasingh<sup>a</sup>, Rupert Kargl<sup>b,c</sup>, Karin Stana Kleinschek<sup>b,d</sup>, Jana Schaubeder<sup>e</sup>, Stefan Spirk<sup>e</sup>, Anna Ström<sup>a</sup>, Tiina Nypelö<sup>a,f,\*</sup>

<sup>a</sup> Department of Chemistry and Chemical Engineering, Chalmers University of Technology, 41296 Gothenburg, Sweden

<sup>b</sup> Institute of Chemistry and Technology of Biobased Systems, Graz University of Technology, 8010 Graz, Austria

<sup>c</sup> Laboratory for Characterization and Processing of Polymers, University of Maribor, 2000 Maribor, Slovenia

<sup>d</sup> University of Maribor, Institute of Automation, Faculty of Electrical Engineering and Computer Science, Koroska cesta 46, 2000 Maribor, Slovenia

<sup>e</sup> Institute of Bioproducts and Paper Technology, Graz University of Technology, 8010 Graz, Austria

<sup>f</sup> Wallenberg Wood Science Center, Chalmers University of Technology, 41296 Gothenburg, Sweden

## ARTICLE INFO

### Keywords:

Quartz crystal microbalance with dissipation monitoring  
Water interactions  
Solubilization

## ABSTRACT

Polysaccharides are excellent network formers and are often processed into films from water solutions. Despite being hydrophilic polysaccharides, the typical xylans liberated from wood are sparsely soluble in water. We have previously suggested that an additional piece to the solubilization puzzle is modification of the xylan backbone via oxidative cleavage of the saccharide ring. Here, we demonstrate the influence of the degree of modification, i. e., degree of oxidation (DO) on xylan solubilization and consequent film formation and stability. Oxidized and reduced wood xylans (i.e., dialcohol xylans) with the highest DO (77 %) within the series exhibited the smallest hydrodynamic diameter ( $d_h$ ) of 60 nm in dimethylsulfoxide (DMSO). We transferred the modified xylans into films credit to their established solubility and then quantified the film water interactions. Dialcohol xylans with intermediate DOs (42 and 63 %) did not form continuous films. The films swelled slightly when subjected to humidity. However, the film with the highest DO demonstrated a significant moisture uptake that depended on the film mass and was not observed with the other modified grades or with unmodified xylan.

## 1. Introduction

Xylans are hemicelluloses composed of D-xylopyranose units linked by  $\beta$ -1,4 glycosidic bonds (Sixta, 2006; Teleman, 2009). They are abundant in hardwoods (15–35 %) and can be liberated from wood in pulping processes or by alkaline and hot water extraction, which decreases their molar mass and modifies their substituting group compositions (Sixta, 2006). Wood xylans are linear polysaccharides and are typically decorated with uronic acids, acetyl groups, and monosaccharide side groups (Teleman, 2009). Arabino(glucurono)xylan and 4-O-methylglucuronoxylan are branched xylans which can be found in some wood species, while other branched xylans such as arabinoxylan and glucurono(arabino)xylan are commonly found in crops and grasses (Ebringerová & Heinze, 2000).

Currently, cellulose is the main product utilized from the forest biomass, whereas the other macromolecules, such as xylans, are not employed in materials engineering. However, the growing recognition that resource efficiency is paramount for supplying renewable materials while preserving the forest as a carbon sink makes xylan use a topic for

consideration.

Wood xylans are hydrophilic due to their abundant hydroxyl groups, but most of the liberated xylans are, in fact, poorly water soluble. Branched polysaccharides are typically more soluble than unbranched polysaccharides; therefore, the removal of the substituents during liberation promotes the close packing of adjacent chains. For example, debranching of arabinoxylan to a degree of substitution of 0.04 rendered it insoluble in water (Bosmans et al., 2014). Charge can efficiently increase water solubility, and xylans contain uronic acid side groups that provide this feature (Guo et al., 2017). Molar mass is another factor that governs solubility, since large molecules promote their self-interaction due to their large volume and reduce conformational freedom with respect to the solvent. For these reasons, many attempts have been made to improve the water solubility of xylan by searching for suitable solvents or xylan modifications.

The search for better solvents has involved new ones, such as ionic liquids (Yu et al., 2020), whereas xylan modifications have included hydroxypropylation (Hettrich et al., 2017; Jain et al., 2000; Nypelö et al., 2016), carboxymethylation (Hettrich et al., 2017), sulfoethylation

\* Corresponding author at: Department of Chemistry and Chemical Engineering, Chalmers University of Technology, 41296 Gothenburg, Sweden.

E-mail address: [tiina.nypelo@chalmers.se](mailto:tiina.nypelo@chalmers.se) (T. Nypelö).

(Ebringerová et al., 1998), and oxidation (Amer et al., 2016) reactions aimed at improving xylan interactions with water. Periodate oxidation has been used for carbohydrate modification and analysis (Malaprade, 1928; Bobbitt, 1956; Zeronian et al., 1964) for decades. Oxidation cleaves the carbon-carbon bonds between C2 and C3 of xylopyranose units and equips those carbons with aldehydes. The newly generated aldehydes are partially converted to hydrated aldehydes and form intra- or interlinkages in solution immediately after the oxidation or in the presence of water. Dialdehyde xylan has been demonstrated to form flexible and transparent films (Rao et al., 2021) and to stabilize liquid metal inks (Hao et al., 2021). The aldehydes can be reduced to more stable forms (i.e., hydroxyl groups) to minimize self-interactions (Börjesson et al., 2018; Leguy et al., 2018). Oxidation is also expected to increase mobility in the chain due to opening of the xylopyranose ring, thereby interrupting the close packing of the chains and increasing the water interactions (Palasingh et al., 2022).

The focus of the present study was to evaluate the influence of the degree of modification, i.e., oxidation (DO) on the dissolution, film formation, and film stability of beechwood xylan following periodate oxidation and sodium borohydride reduction. The hypotheses were that these modifications enable xylan dissolution in solvents that allow film formation, and that the modifications further increase the film's attractive interaction with water. The characteristics of the dialcohol xylan (DalX) products in solution and the humidity sensitivity of the thin films were investigated.

## 2. Materials and methods

Beechwood xylan, sodium periodate, sodium borohydride, ethylene glycol, sulfuric acid, calcium chloride, sodium chloride, potassium sulfate, and dimethyl sulfoxide (DMSO) were purchased from Sigma Aldrich (Sweden) and used without further purification. Oxidation (Fig. 1) was conducted according to Amer et al. (2016). Xylan (4 g) was dispersed in 115 ml of ultrapure water overnight, heated to 70 °C for 30 min, and cooled to room temperature before starting the reaction. Sodium periodate solution was prepared by dissolving 2.2 to 5.2 g of sodium periodate in 75 ml of ultrapure water, and the entire volume was added to the xylan solution. The oxidation was performed in darkness at room temperature for 24 h. The DO was measured by observing the consumption of periodate ions by UV–Vis spectroscopy (Cary 60 UV–Vis Spectrophotometer, Agilent) (Maekawa et al., 1986). Unreacted periodate was quenched with ethylene glycol (1 ml). The resulting oxidized xylyns were dialyzed in water for 2 days and then reduced with sodium borohydride (2 g; 1:2 anhydroxylose unit mole equivalent) for 2 days to obtain dialcohol xylan (DalX). The DalX was purified by dialysis for 2 days (Fig. 1), and then freeze-dried and stored in a freezer.

### 2.1. Carbohydrate composition

Xylan was hydrolyzed using 72 % sulfuric acid and treatment at 125 °C for 1 h (Theander & Westerlund, 1986). In short, 0.45 ml 72 % sulfuric acid was added to 30 mg xylan and placed under vacuum for 15 min. The suspension was then placed in 30 °C water bath for 1 h, followed by dilution with 12.6 g deionized water and autoclaving at 125 °C

for 1 h. The hydrolysate was filtered through a glass microfiber filter and diluted to 25 ml total volume with deionized water. A fucose standard (2 ml of 200 mg/l solution) was added to 1 ml hydrolysate, and subsequently diluted (1:50, v/v). The solution was filtered through a 0.2 µm PVDF filter. The carbohydrate composition was analyzed by high performance anion exchange chromatography with pulsed amperometric detection (Dionex ICS-3000 equipped with CarboPac PA1 analysis column, Dionex Corporation, USA). The system was operated using NaOH/NaAcOH and NaOH eluents.

### 2.2. Uronic acid determination

Uronic acid content of the xylan was determined using a colorimetric method with UV–Vis spectroscopy (Blumenkrantz & Asboe-Hansen, 1973). Xylan (10 mg) was hydrolyzed with 0.5 ml 96 % cold sulfuric acid and stirred with vortex for 5 min. Then, 0.25 ml cold water was added and was stirred for 5 min. These steps were repeated one more time. The hydrolysate was then diluted twice: firstly, with water to 10 ml total volume and secondly, 3 times dilution with 9:1 water to sulfuric acid solution. Diluted hydrolysate (160 µl), sulfamic acid-potassium sulfamate (20 µl) and sodium tetraborate in sulfuric acid (800 µl) were mixed in plastic vial and treated at 95 °C for 20 min. The solution was analyzed with UV–Vis spectroscopy after addition of 40 µl of 0.15 % w/v 3-phenylphenol.

### 2.3. Size exclusion chromatography (SEC)

The molar mass and dispersity of the beechwood xylan and DalXs were investigated using DMSO-based SEC system equipped with a Jordi xStream GPC column (Jordi Labs, MA, USA) and analyzed using refractive index (RI) and right-angle light scattering (RALS, 670 nm, 90°) detectors. Approximately 4 mg of xylan and DalXs was pre-swollen in 30 µl of water overnight prior to dissolution in 2 ml of 0.01 M LiBr/DMSO. The solutions were prepared at room temperature and then filtered through a 0.45 µm PTFE syringe filter before analyzing. The filtered solutions (100 µl) were injected into the SEC system, The column temperature was 60 °C, the detector temperature was 40 °C, and the flow rate was 0.8 ml/min.

### 2.4. Dynamic light scattering (DLS)

The hydrodynamic diameter ( $d_h$ ) of DalX in DMSO was determined by DLS. Xylan and DalXs solutions at concentrations of 5 mg/ml were prepared by pre-swelling 10 mg of xylan and DalXs in 30 µl ultrapure water overnight before adding DMSO. The solutions were analyzed with a Litesizer™ 500 (Anton Paar, Austria) at 25 °C. The  $d_h$  was calculated using the Stokes–Einstein equation (Eq. (1)):

$$d_h = \frac{kT}{3\pi\eta D} \quad (1)$$

where  $k$  is Boltzmann's constant,  $T$  is absolute temperature,  $\eta$  is viscosity, and  $D$  is a transitional diffusion coefficient. The number distribution and diffusion coefficient were determined using the Kalliope™ v2.20.2 software. The viscosity of DMSO was 0.00199 Pa·s at 25 °C

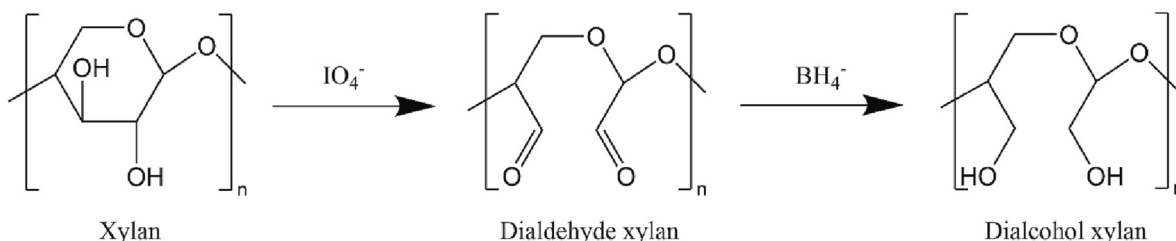


Fig. 1. Periodate oxidation and borohydride reduction of xylan.

(LeBel & Goring, 1962).

## 2.5. Film formation

Xylan and DalXs (10 mg) were pre-swollen in 30  $\mu$ l ultrapure water and then dissolved in DMSO at a concentration of 5 mg/ml. The solutions were formed into films on silicon substrates (Sievert wafers, Germany) and on commercial silicon dioxide-coated Quartz crystal microbalance with dissipation (DCM-D) sensors (Quartz Pro, Sweden) by spin coating using a POLOS SPIN 200i device (SPS-Europe B.V., Netherlands) or a WS-650MZ-23NPP device (Laurell Technologies Corporation, USA) operated at 4000 rpm for 180 s. Two layers of films were deposited to ensure full coverage of the film. The films were then heated in an oven at 80  $^{\circ}$ C for 10 min and stored in a desiccator. The silicon substrates were used for morphology observations and thickness determinations, while the QCM-D sensors were used for film humidity sensitivity and thickness determinations.

## 2.6. Quartz crystal microbalance with dissipation

A QCM-D instrument (Q-Sense E4 equipped with QFM 401 flow module, Biolin Scientific AB, Sweden) was used to determine film thickness and to investigate the film response to humidity. The film mass was determined according to Tammelin et al. (2015). In brief, the resonance frequency of the sensor before and after film deposition was recorded. The mass ( $\Delta m$ ) was extracted using the Sauerbrey equation (Eq. (2)).

$$\Delta m = -C \frac{\Delta f}{n} \quad (2)$$

Where  $C$  is the sensor sensitivity constant (0.177 mg/(Hz  $m^2$ )),  $\Delta f$  is the frequency shift after film deposition, and  $n$  is an overtone number (3, 5, 7, ..., 11). The thickness of the film ( $d$ ) was calculated based on the assumed density ( $\rho$ ) of 1200 kg/ $m^3$  for xylan and dialcohol xylan films (Eq. (3)).

$$d = \frac{\Delta m}{\rho} \quad (3)$$

Swelling of the films was investigated by pumping air onto the film at a specific relative humidity (RH) generated by saturated salt solutions. The  $CaCl_2$ , NaCl, and  $K_2SO_4$  salt solutions (100 ml) were prepared in 250 ml flasks. The RH level generated by the salt solution inside the flask was monitored with an RH sensor. A baseline was obtained by feeding dry air (6 %RH; produced by pumping air through  $CaCl_2$ ) overnight at a flow rate of 400  $\mu$ l/min. The films were exposed to 26 %RH, 75 %RH, or 97 %RH for 90 min and then cycled back to dry air. The experiments were performed at room temperature (25  $^{\circ}$ C). Mass changes were calculated with the Sauerbrey equation (Eq. (2)).

## 2.7. Atomic force microscopy (AFM)

The morphology, thickness, and surface roughness of the xylan and DalX films were investigated using AFM (NTEGRA AFM, NT-MDT, Russia) with Tap300Al-G tips (BudgetSensors, Bulgaria). The morphology and roughness of the films were scanned using tapping mode in at least 3 different positions. The data were processed using Gwyddion software version 2.60. The thickness was determined by scratching the films with a sharp tool to partly remove the film from the substrates, and the scans were then recorded across the scratch. The difference in the height of the substrate (scratched area) and the film (unscratched area) was taken as the thickness of the film.

## 3. Results and discussion

### 3.1. Oxidation and reduction of xylan

Beechwood xylan had a relative monosaccharide composition of >99 wt% xylose and an uronic acid content of 8 mol%. A weight average molecular mass of the xylan was 14,000 g/mol with dispersity of 2.5. The oxidation led to DOs of 42 %, 63 %, and 77 % (denoted DalX40, DalX60, and DalX80, respectively). Their measured molar masses and dispersities were 14,500, 12,000, and 10,500 g/mol and 2.8, 2.8, and 2.5, respectively. A higher periodate concentration led to a faster reaction (Fig. 2). With all three tested reactant-to-xylan ratios, most of the periodate was consumed during the first 6 h. Nevertheless, a high DO gave a low yield due to degradation (30 % yield), while the DalX60 and DalX40 yields were 49 % and 70 %, respectively.

### 3.2. Solubilization of dialcohol xylans

The oxidation was anticipated to improve the attractive interaction of xylan with polar solvents. Opening of the xylose units at the backbone was expected to interrupt the close packing of the chains and enable solvent access. We have previously shown that beechwood dialcohol xylan dissolved in water at a concentration of 20 mg/ml with 84 % DO (Palasingh et al., 2022). Here, the modified xylans did not completely solubilize in water but solubilized better than the unmodified xylan, as observed by the naked eye (Fig. S1). The solutions of modified xylans were turbid at 5 mg/ml, suggesting that aggregates were formed. Hence, complete solubilization was not observed, and although periodate oxidation and reduction improved the solubilization of xylan in water, they were not sufficient to fully solubilize xylan. The explanation for the difference compared to previously reported water-soluble DalX (Palasingh et al., 2022) may be that the uronic acid content was lower in the xylan used here (8 mol% compared to 12 mol%) which contributed to its poor solubilization.

However, both the xylan and the DalXs were soluble in DMSO, which has been shown to be a good solvent for xylans (Ebringerová et al., 1994). The hydrodynamic diameter;  $d_h$ , determined by measuring the rate of scattered light intensity fluctuation, revealed a monomodal size distribution (Fig. 3a). The average hydrated size determined from the number weighted distribution was nearly identical for unmodified xylan

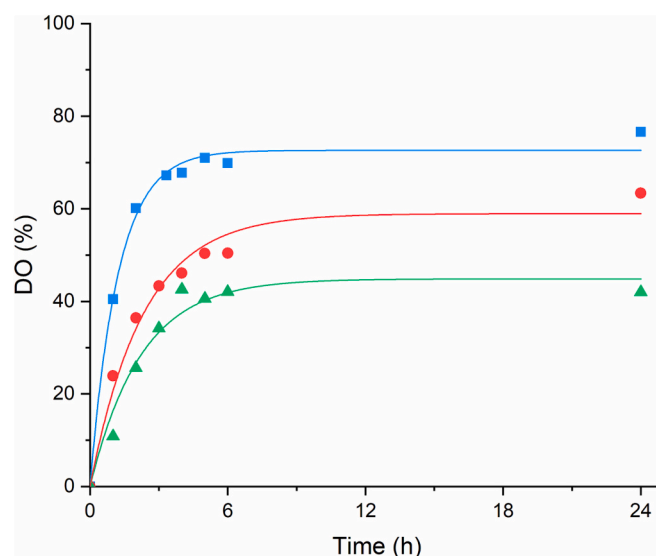
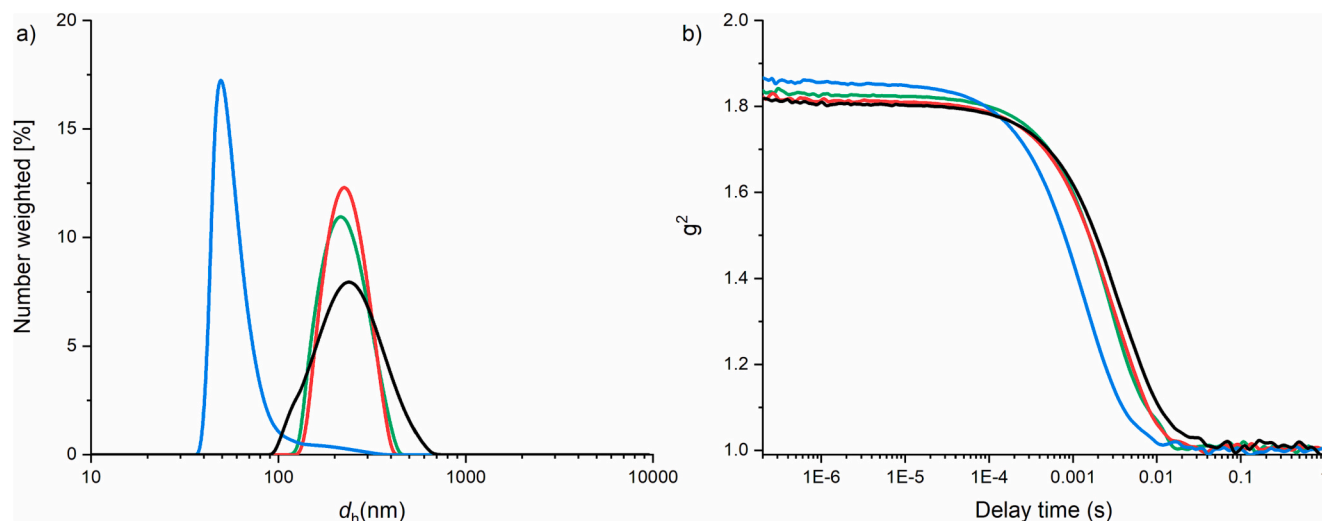


Fig. 2. Progress of periodate oxidation of xylan to 42 % (green triangles), 63 % (red circles), and 77 % (blue squares) DO. The reaction was fitted with a first-order kinetic model. (For interpretation of the references to color in this figure legend, the reader is referred to the web version of this article.)





**Fig. 3.** Hydrodynamic diameter ( $d_h$ ) (a) and correlation function (b) of xylan (black), DalX40 (green), DalX60 (red), and DalX80 (blue) dissolved in DMSO at a concentration of 5 mg/ml. (For interpretation of the references to color in this figure legend, the reader is referred to the web version of this article.)

(205 nm), DalX60 (224 nm), and DalX40 (208 nm) at 5 mg/ml. However, the native xylan exhibited a wider size distribution than the modified grades. Conversely, the  $d_h$  of DalX80 was 3 times smaller (60 nm). This implies that a DO larger than 63 % is required to decrease the  $d_h$ . Nevertheless, the distribution of DalX80 still showed traces of large aggregates over 100 nm, which probably reflected heterogeneous oxidation due to poor xylan dispersion. The autocorrelation function ( $g^2$ ) represents the similarity of the intensity profile at time  $t_0$  and  $t$  and implies the particle size by the signal decay. If the particles are small, they move rapidly, leading to a fast decay of the degree of similarity, as can be observed for DalX80 in Fig. 3b, compared to the other grades.

### 3.3. Morphology of the dialcohol xylan films

The topography and morphology of thin films formed from DMSO-based solutions of xylan and DalXs at 5 mg/mL via spin coating was investigated by AFM (Fig. 4). The morphology of the unmodified xylan films exhibited fractal patterns, resembling phase-separated polymer films (Fig. 4a). The films consisted of spherical features that assembled into an open film with 45 % surface coverage. As the DO increased, the film openness expanded and island-shaped areas grew larger (Fig. 4b–c). We note that DalX40 and DalX60 films were inhomogeneous, since they showed areas with denser islands and some with larger islands and surface coverage decreased to 30 % and 35 % for DalX40 and DalX60, respectively. DalX80 produced homogeneous closed and smooth films, where the surface consisted of small features (Fig. 4d), similar to those of water-soluble xylan (Kishani et al., 2019). The surface roughness of DalX80 was  $0.6 \pm 0.4$  nm, while a value for the open films is not reported as the roughness is not representing the accurate film surface roughness. Neat xylan films (Peng et al., 2011; Saxena et al., 2009) and

xylan on cellulose substrates (Dalvi et al., 2020; Ganser et al., 2016) prepared from aqueous solutions have been reported to form a nodular pattern, which probably originates from the aggregation in solution, as observed here as well.

The film thickness was examined using two approaches: recording the height difference between the film and the substrate using AFM, and deriving the thickness through film mass using QCM-D. The thickness of the full coverage DalX80 film from AFM analysis was  $9.6 \pm 2.0$  nm, while analysis using QCM-D indicated only half the thickness ( $4.6 \pm 1.5$  nm) compared to the values derived from AFM. The AFM method probes the thickness directly using the morphology scan, whereas the QCM-D thickness value is derived from modeling and an assumption of layer density; this difference could in part explain the difference in thickness values. However, no technique currently available is superior to determine thickness for soft biopolymer films without a compromise (Spirk et al., 2021). Hence, we provide the findings of the two methods and a guide to use them qualitatively, while recommending a comparison of values from the same analysis only. The open film thickness was analyzed only with AFM and the thickness was  $9.4 \pm 2.4$  nm,  $5.2 \pm 1.4$  nm and  $6.0 \pm 2.2$  nm for xylan, DalX40 and DalX60, respectively.

### 3.4. Interaction of the films with humid air

The xylan films were subjected to varying humidity levels up to nearly saturated conditions (97 %RH) in a QCM-D chamber. The humidity response of the films increased with increasing humidity levels, and more water was incorporated into the films (Fig. 5a–d). In theory, the film mass has a direct influence on water vapor uptake as more molecules are available. While the xylan and DalX40 films did not follow this concept (Fig. 5a and b, respectively), DalX80 demonstrated an

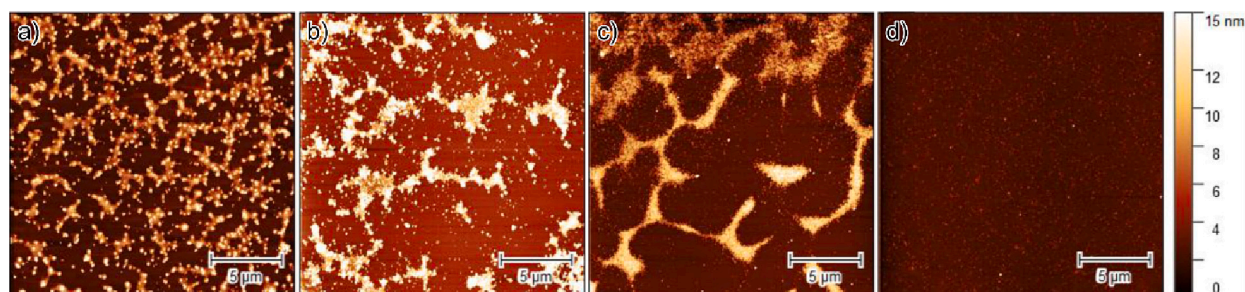


**Fig. 4.** AFM topography images of xylan (a), DalX40 (b), DalX60 (c), and DalX80 (d) film on a substrate.

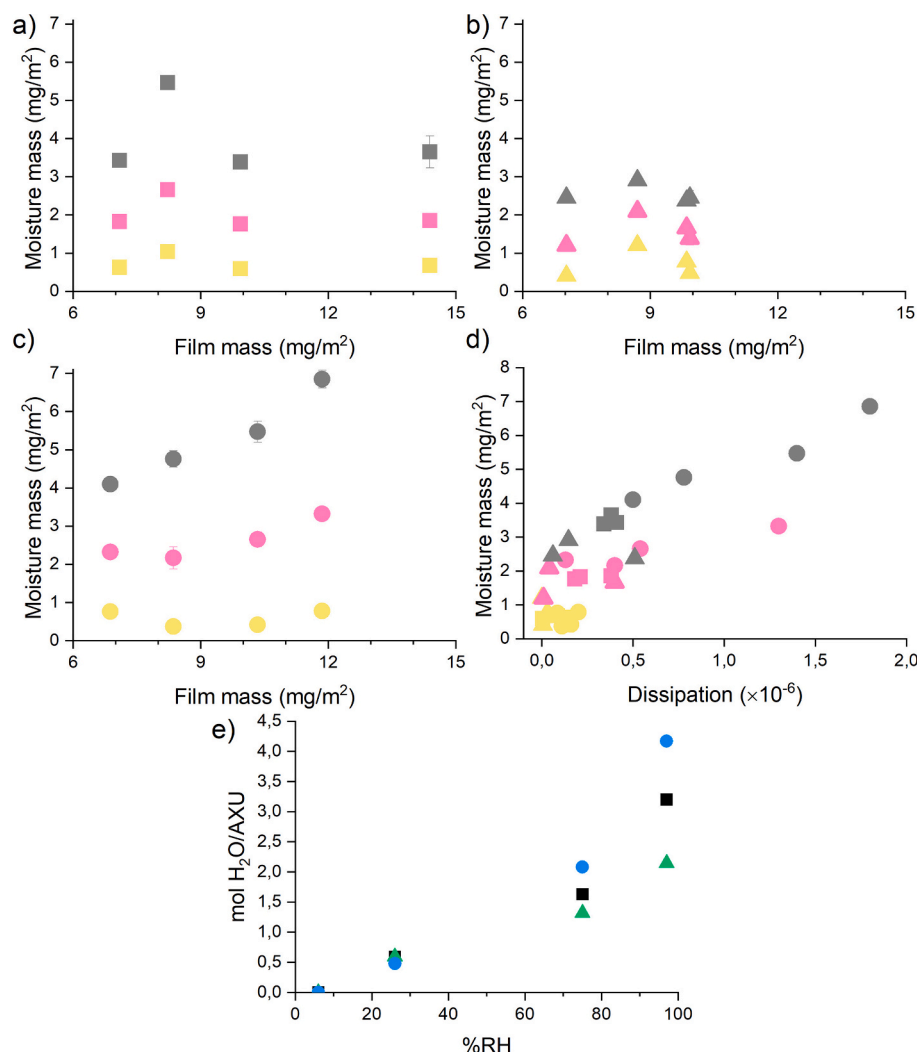


**Fig. 5.** Moisture adsorbed on xylan (a), DalX40 (b) and DalX80 (c) films as a function of film mass in 26 %RH (yellow), 75 %RH (pink), and 97 %RH (gray). Amount of the adsorbed moisture adsorbed as a function of dissipation (d) of xylan (squares), DalX40 (triangles) and DalX80 (circles). The resulting molecules of water per AXU at different humidity levels of xylan (black squares), DalX40 (green triangles) and DalX80 (blue circles) (e). (For interpretation of the references to color in this figure legend, the reader is referred to the web version of this article.)

increasing water vapor uptake per film mass (Fig. 5c).

The viscoelasticity of the films during adsorption was investigated by plotting the moisture mass versus the energy dissipation (Fig. 5d), where dissipation is indicative of the film viscoelasticity (i.e., softness). At 26 % RH, the dissipation of the xylan and DalX40 films was almost unaltered, whereas the dissipation of DalX80 films slightly increased. However, the values were low, with little practical significance. The expectation was that moisture bound in the film would amplify the viscous component and result in an increase in the dissipation value. Increasing the RH to 75 % did not change the dissipation of xylan and DalX40 films very much, whereas the DalX80 films became more viscous, as indicated by the increase in the dissipation value. At the highest RH, the dissipation value for the DalX80 films was obviously increased. This behavior was similar to that of amorphous cellulose films, where RH up to 75 % has been shown to lead to a small dissipation increase ( $1 \times 10^{-6}$  or lower) that further increased at 97 %RH (Tammelin et al., 2015). Arabinoglucuronoxylan films (Escalante et al., 2012) have been reported to exhibit increasing softness at 80 %RH.

Since the film mass was determined by the QCM-D method, it is possible to make a correlation of the hydration of the xylan films at the different humidity levels at the molecular level. For this purpose, the mass of the deposited film and the water needs to be converted into moles, i.e., simply dividing the deposited xylan mass by the molar mass of the anhydroxylose unit (132.14 g/mol) and by dividing the water mass by 18.01 g/mol. Upon dividing the moles of water by the moles of AXU gives then the ratio of water molecules per AXU. The amount of

incorporated water per AXU was between 0.48 and 0.59 for the different films at 26 %RH (i.e., at these levels, two AXUs absorb a single water molecule statistically) (Fig. 5e). At higher humidity levels (75 %RH), the films exhibit a much more intense interaction, with the largest value of 1.3 to 2.0 molecules absorbing per AXU (DO 77 %). At 97 %RH, the DalX80 film was capable of absorbing 4.2 molecules of water per AXU, while the DalX40 and the xylan film showed less interaction (2.3 and 3.1 water molecules per AXU, respectively). The oxidation seems to need to reach a certain degree to enhance the water vapor adsorption above that of the neat xylan films. At the highest humidity levels, the DalX film behave similarly to cellulose films, where in such experiments 1.08 to 3.6 water molecules were absorbed in 75 and 97 %RH (Reishofer et al., 2022). Water vapor incorporation into cellulose thin films was similar at low humidity levels, regardless of the film type. At low humidity levels, the effect of morphology and supramolecular arrangement of the macromolecule chains in the films did not play a prominent role. The chemistry is important for such interactions as well but the difference of oxidized xylans and neat xylans at low humidity levels (i.e. 26 %RH) is within the accuracy limits of the method and does not seem to play a role neither. By increasing the humidity levels, however, both effects, morphology/arrangements and chemistry increasingly impact the water vapor uptake in the films. Any change in the supramolecular arrangement has then a tremendous effect on water vapor uptake was demonstrated at the example of cellulose thin films. There, thermal treatment of the thin films led to an aggregation of cellulose macromolecules (Ehmann et al., 2015). Consequently, both liquid water uptake (Kittl

et al., 2011; Kontturi et al., 2013; Mohan et al., 2012) as well as water vapor uptake was much lower than for the nontreated thin films (e.g. water uptake 2.0 vs 3.6 molecules of H<sub>2</sub>O/AGU for dried and nontreated surfaces) (Reishofer et al., 2022). An overview on these findings on cellulose thin films is summarized in a review article (Kontturi & Spirk, 2019). At high humidity levels, water absorption in nanoconfined pores takes place, and this is a possible explanation, apart from chemistry, for the different humidity response of the films (Reishofer et al., 2022).

The effect of morphology of the xylan films representing islands (all surfaces except DalX80), raises questions whether the water uptake mechanisms in such islands differs from that of the homogenous films. A systematic study is needed to address this question, which requires the use of e.g., sophisticated nano-IR grazing incidence mapping experiments which would show whether water sits on the surface, at the interface to the silicon substrate and xylan or whether it is distributed equally over the islands. From the data we collected it seems that the aggregates formed on the surfaces restrict access of water inside the material, probably due to minimization of the surface free energy. This would make the incorporation of water a thermodynamically unfavored process.

#### 4. Conclusions

Periodate oxidation and borohydride reduction modification changed beechwood xylan structure by opening the xylose unit at the backbone; this was expected to promote xylan solubilization in water and consequently film formation from the solution. The unbranched beechwood xylan required a high DO (77 %) to allow its solubilization in water. In DMSO, the high DO xylan displayed the lowest hydrodynamic diameter among the grades inspected and produced homogeneous smooth films. These films swelled with increasing relative humidity and their energy dissipation value obviously increased. We conclude that the modification of xylan into DalX80 transformed it more solubilizable, and that enabled film formation from the solution. This grade also exhibited a high hydration per AXU units and confirms that the modification can provide tailor-made xylans, and films thereof, with defined water uptake capabilities.

#### CRedit authorship contribution statement

CP: Experimental work and writing the original draft, reviewing and editing. RK, KSK: Supervision and planning of QCM-D experiments, writing, reviewing, editing. JS: DLS measurements and analysis, writing, reviewing, editing. SS: Data analysis, writing, reviewing, editing. AS: Conceptualization, writing, reviewing, editing. TN: Conceptualization, writing, reviewing, editing.

#### Declaration of competing interest

The authors declare that they have no known competing financial interests or personal relationships that could have appeared to influence the work reported in this paper.

#### Data availability

Data will be made available on request.

#### Acknowledgements

We thank the following for funding our research: Swedish Research Council grant (registration number 2017-05138), Nordic Council of Ministers (Joint Nordic project SNS Hemisurf 127), Wallenberg Wood Science Center and the Materials Science Area of Advance at Chalmers. We would like to thank Jakob Karlsson for assisting with uronic acid determination. We acknowledge the Division of Forest Products and Chemical Engineering at Chalmers for access to carbohydrate analysis

facilities. We acknowledge Felix Abik and Kirsi S. Mikkonen at Helsinki University for the molar mass analysis. We would like to thank Florian Lackner from Graz University of Technology for constructing the humidity sensing device for the QCM-D measurements.

#### Appendix A. Supplementary data

Supplementary data to this article can be found online at <https://doi.org/10.1016/j.carbpol.2023.120810>.

#### References

- Amer, H., Nypelö, T., Sulaeva, I., Bacher, M., Henniges, U., Potthast, A., & Rosenau, T. (2016). Synthesis and characterization of periodate-oxidized polysaccharides: Dialdehyde xylan (DAX). *Biomacromolecules*, 17(9), 2972–2980.
- Blumenkrantz, N., & Asboe-Hansen, G. (1973). New method for quantitative determination of uronic acids. *Analytical Biochemistry*, 54(2), 484–489.
- Bobbitt, J. (1956). Periodate oxidation of carbohydrates. In *Advances in carbohydrate chemistry* (pp. 1–41). Elsevier.
- Börjesson, M., Larsson, A., Westman, G., & Ström, A. (2018). Periodate oxidation of xylan-based hemicelluloses and its effect on their thermal properties. *Carbohydrate Polymers*, 202, 280–287.
- Bosmans, T. J., Stépán, A. M., Toriz, G., Renneckar, S., Karabulut, E., Wågberg, L., & Gatenholm, P. (2014). Assembly of debranched xylan from solution and on nanocellulosic surfaces. *Biomacromolecules*, 15(3), 924–930.
- Dalvi, L. C., Laine, C., Virtanen, T., Liitiä, T., Tenhunen, T.-M., Orelma, H., Tammelin, T., & Tamminen, T. (2020). Study of xylan and cellulose interactions monitored with solid-state NMR and QCM-D. *Holzforschung*, 74(7), 643–653.
- Ebringerová, A., & Heinze, T. (2000). Xylan and xylan derivatives—biopolymers with valuable properties. 1. Naturally occurring xylans structures, isolation procedures and properties. *Macromolecular Rapid Communications*, 21(9), 542–556.
- Ebringerová, A., Hromádková, Z., Burchard, W., Dolega, R., & Vorwerg, W. (1994). Solution properties of water-insoluble rye-bran arabinoxylan. *Carbohydrate Polymers*, 24(3), 161–169.
- Ebringerová, A., Sroková, I., Talába, P., Kačuráková, M., & Hromádková, Z. (1998). Amphiphilic beechwood glucuronoxylan derivatives. *Journal of Applied Polymer Science*, 67(9), 1523–1530.
- Ehmann, H. M. A., Werzer, O., Pachmajer, S., Mohan, T., Amenitsch, H., Resel, R., Kornherr, A., Stana-Kleinschek, K., Kontturi, E., & Spirk, S. (2015). Surface-sensitive approach to interpreting supramolecular rearrangements in cellulose by synchrotron grazing incidence small-angle X-ray scattering. *ACS Macro Letters*, 4(7), 713–716.
- Escalante, A., Gonçalves, A., Bodin, A., Stepan, A., Sandström, C., Toriz, G., & Gatenholm, P. (2012). Flexible oxygen barrier films from spruce xylan. *Carbohydrate Polymers*, 87(4), 2381–2387.
- Ganser, C., Niegellhell, K., Czibula, C., Chemelli, A., Teichert, C., Schennach, R., & Spirk, S. (2016). Topography effects in AFM force mapping experiments on xylan-decorated cellulose thin films. *Holzforschung*, 70(12), 1115–1123.
- Guo, M. Q., Hu, X., Wang, C., & Ai, L. (2017). Polysaccharides: Structure and solubility. In *Solubility of polysaccharides* (pp. 8–21). IntechOpen.
- Hao, X., Li, N., Wang, H., Jia, S., Liu, Q., & Peng, F. (2021). Dialdehyde xylan-based sustainable, stable, and catalytic liquid metal nano-inks. *Green Chemistry*, 23(19), 7796–7804.
- Hettrich, K., Drechsler, U., Loth, F., & Volkert, B. (2017). Preparation and characterization of water-soluble xylan ethers. *Polymers*, 9(4), 129.
- Jain, R. K., Sjöstedt, M., & Glasser, W. G. (2000). Thermoplastic xylan derivatives with propylene oxide. *Cellulose*, 7(4), 319–336.
- Kishani, S., Escalante, A., Toriz, G., Vilaplana, F., Gatenholm, P., Hansson, P., & Wågberg, L. (2019). Experimental and theoretical evaluation of the solubility/insolubility of spruce xylan (arabino glucuronoxylan). *Biomacromolecules*, 20(3), 1263–1270.
- Kittle, J. D., Du, X., Jiang, F., Qian, C., Heinze, T., Roman, M., & Esker, A. R. (2011). Equilibrium water contents of cellulose films determined via solvent exchange and quartz crystal microbalance with dissipation monitoring. *Biomacromolecules*, 12(8), 2881–2887.
- Kontturi, E., & Spirk, S. (2019). Ultrathin films of cellulose: A materials perspective. *Frontiers in Chemistry*, 7(488).
- Kontturi, K. S., Kontturi, E., & Laine, J. (2013). Specific water uptake of thin films from nanofibrillar cellulose. *Journal of Materials Chemistry A*, 1(43), 13655–13663.
- LeBel, R. G., & Goring, D. A. I. (1962). Density, viscosity, refractive index, and hygroscopicity of mixtures of water and dimethyl sulfoxide. *Journal of Chemical & Engineering Data*, 7(1), 100–101.
- Leguy, J., Diallo, A., Pataux, J.-L., Nishiyama, Y., Heux, L., & Jean, B. (2018). Periodate oxidation followed by NaBH<sub>4</sub> reduction converts microfibrillated cellulose into sterically stabilized neutral cellulose nanocrystal suspensions. *Langmuir*, 34(37), 11066–11075.
- Maekawa, E., Kosaki, T., & Koshijima, T. (1986). Periodate oxidation of mercerized cellulose and regenerated cellulose. In *Wood Research Institute* (pp. 44–49). Kyoto University.
- Malaprade, L. (1928). Oxidation of some polyalcohols by periodic acid—Applications. *Comptes Rendus*, 186, 382–384.

- Mohan, T., Spirk, S., Kargl, R., Doliška, A., Vesel, A., Salzmann, I., Resel, R., Ribitsch, V., & Stana-Kleinschek, K. (2012). Exploring the rearrangement of amorphous cellulose model thin films upon heat treatment. *Soft Matter*, 8(38), 9807–9815.
- Nypelö, T., Laine, C., Aoki, M., Tammelin, T., & Henniges, U. (2016). Etherification of wood-based hemicelluloses for interfacial activity. *Biomacromolecules*, 17(5), 1894–1901.
- Palasingh, C., Nakayama, K., Abik, F., Mikkonen, K. S., Evenäs, L., Ström, A., & Nypelö, T. (2022). Modification of xylan via an oxidation–reduction reaction. *Carbohydrate Polymers*, 292, 119660.
- Peng, X.-W., Ren, J.-L., Zhong, L.-X., & Sun, R.-C. (2011). Nanocomposite films based on xylan-rich hemicelluloses and cellulose nanofibers with enhanced mechanical properties. *Biomacromolecules*, 12(9), 3321–3329.
- Rao, J., Lv, Z., Chen, G., Hao, X., Guan, Y., Peng, P., Su, Z., & Peng, F. (2021). Constructing a novel xylan-based film with flexibility, transparency, and high strength. *Biomacromolecules*, 22(9), 3810–3818.
- Reishofer, D., Resel, R., Sattelkow, J., Fischer, W. J., Niegelhell, K., Mohan, T., Kleinschek, K. S., Amenitsch, H., Plank, H., & Tammelin, T. (2022). Humidity response of cellulose thin films. *Biomacromolecules*, 23(3), 1148–1157.
- Saxena, A., Elder, T. J., Pan, S., & Ragauskas, A. J. (2009). Novel nanocellulosic xylan composite film. *Composites Part B: Engineering*, 40(8), 727–730.
- Sixta, H. (2006). *Handbook of pulp*. Wiley-VCH.
- Spirk, S., Palasingh, C., & Nypelö, T. (2021). Current opportunities and challenges in biopolymer thin film analysis—Determination of film thickness. *Frontiers in Chemical Engineering*, 2021, Article 755446.
- Tammelin, T., Abburi, R., Gestranus, M., Laine, C., Setälä, H., & Österberg, M. (2015). Correlation between cellulose thin film supramolecular structures and interactions with water. *Soft Matter*, 11(21), 4273–4282.
- Teleman, A. (2009). Hemicelluloses and pectins. In M. Ek, G. Gellerstedt, & G. Henriksson (Eds.), *Pulp and paper chemistry and technology - Wood chemistry and biotechnology* (Volume 1). Berlin/Boston, Germany: De Gruyter.
- Theander, O., & Westerlund, E. A. (1986). Studies on dietary fiber. 3. Improved procedures for analysis of dietary fiber. *Journal of Agricultural and Food Chemistry*, 34(2), 330–336.
- Yu, H., Xue, Z., Lan, X., Liu, Q., Shi, R., & Mu, T. (2020). Highly efficient dissolution of xylan in ionic liquid-based deep eutectic solvents. *Cellulose*, 27(11), 6175–6188.
- Zeronian, S., Hudson, F., & Peters, R. (1964). The mechanical properties of paper made from periodate oxycellulose pulp and from the same pulp after reduction with borohydride. *Tappi*, 47, 557–564.